frontiers | Frontiers in Materials

TYPE Original Research
PUBLISHED 17 December 2024
DOI 10.3389/fmats.2024.1532067

OPEN ACCESS

EDITED BY
Xiangdong Liu,
Chinese Academy of Sciences (CAS), China

REVIEWED BY
Jie Zhao,
Jilin University, China
Dongjie Zhang,
Harbin Institute of Technology, China

*CORRESPONDENCE
Yinglu Sun,
ylsun@ciac.ac.cn
Dengzun Yao,
yaodengzun@csei.org.cn
Xianghai Jing,
aerosun@aliyun.com

RECEIVED 21 November 2024
ACCEPTED 02 December 2024
PUBLISHED 17 December 2024

CITATION
Fu M, Hu J, Zhang X, Wang C, Liu Y, Niu J, Sun Y, Yao D and Jing X (2024) Preparation and properties of vanillin-based polyurethane materials for body temperature self-healing. *Front. Mater.* 11:1532067. doi: 10.3389/fmats.2024.1532067

Preparation and properties of vanillin-based polyurethane materials for body temperature self-healing

Mingfu Fu[1], Jiangfeng Hu[1], Xiaochun Zhang[2], Chaozhang Wang[3], Yang Liu[1], Jianzhuang Niu[1], Yinglu Sun[4]*, Dengzun Yao[5]* and Xianghai Jing[6]*

[1]Pipe China West Pipeline Company, Urumqi, China, [2]Production Department of Pipe China, Beijing, China, [3]Pipe China Gansu Pipeline Company, Lanzhou, China, [4]CAS Key Laboratory of High-Performance Synthetic Rubber and Its Composite Materials, Changchun Institute of Applied Chemistry, Chinese Academy of Sciences, Changchun, China, [5]China Special Equipment Inspection and Research Institute, Beijing, China, [6]Lianyungang Jingwei Composite New Materials Co., Ltd., Lianyungang, China

It is difficult to obtain sustainable and fast self-healing polyurethane materials with excellent mechanical properties at low-temperature. In this work, we prepared a series of bio-based polyurethane materials were synthesized with HMDI, Polytetramethylene ether glycol and a vanillin-based chain extender containing dynamic imine bonds. By adjusting the ratio of soft and hard segments, As the content of hard segments increased, the storage modulus and tensile strength of the material increased, the elongation at break decreased, and the heat resistance improved. The results showed that this advanced polyurethane displayed excellent mechanical and self-healing properties due to the presence of a large number of hard segment structures with dynamic imine bonds. Moreover, the tight arrangement of hydrogen bonds can promote the exchange of dynamic imine bonds and endow the material with body-temperature self-healing ability. It can recover to 98% of its original stress in 20 min at 36°C.

KEYWORDS

vanillin-based polyurethane, microphase separation, self-healing, body temperature, imine bond

1 Introduction

Inspired by the inherent self-healing characteristics of organic organisms in nature, bionic intelligent self-repairing materials synthesized based on physical or chemical strategies have been extensively studied in recent years (Li et al., 2018; Diesendruck et al., 2015). These materials can effectively extend the service life of functional polymer materials (Zhang et al., 2021). Researchers have successfully prepared various new types of intelligent polymer materials that can spontaneously and rapidly repair at room temperature, and have effectively explored their potential application value in different fields. Body temperature self-healing material is an intelligent material that can achieve self repair under conditions close to human body temperature. This characteristic makes

it widely applicable in tissue repair, bioelectronics and other fields (Yan et al., 2024; Jiang et al., 2021; Chen et al., 2023).

Polyurethane materials are widely used in various fields such as industry and biomedicine due to their excellent mechanical, physical, and chemical properties, as well as good biocompatibility (Yan et al., 2024; Dong et al., 2021). With the development of dynamic bonds, research on healable and self-repairing polyurethanes based on dynamic covalent bonds has been continuously emerging. These dynamic covalent bonds include disulfide bonds (Nevejans et al., 2019; Nevejans et al., 2016), Diels–Alder bonds (Ratwani et al., 2023; Maeda et al., 2009), imine bonds (Su et al., 2020; Alabiso and Schlogl, 2020), *etc.*, which can repair material damage through exchange mechanisms. The team led by Professor Zhengwei You has designed a polyurethane elastomer with excellent spontaneous self-healing properties under physiological conditions (Jiang et al., 2021). This material can replace sutures and metal wires in traditional abdominal aortic aneurysm, nerve conjoining, and sternum fixation surgical treatments, effectively avoiding secondary damage to the lesion site and surrounding tissues caused by surgery (Yan et al., 2024).

Polyurethane is different from olefin based polymers in that its molecular structure is composed of soft segments (oligomeric polyols) and hard segments (polyisocyanates, chain extenders or crosslinkers, *etc.*), resulting in strong designability of polyurethane (Akindoyo et al., 2016; Javni et al., 2015). Isocyanates with different chemical structures, oligomeric polyols with different molecular weights, different types of small molecule diols or diamines, branching and crosslinking, adjusting their ratios or preparation sequences, *etc.*, which can all have a significant impact on the properties of the product (Akindoyo et al., 2016; Javni et al., 2015). HMDI is a fatty ring isocyanate. Wu et al. prepared a series of self-healing polyurethanes and studied the effect of hard segment types on the mechanical properties and self-healing efficiency of polyurethanes (Wu et al., 2021). They demonstrated that polyurethanes containing HMDI give TPU higher mechanical properties without affecting the repair performance. PTMG is an amorphous polyol with excellent low-temperature flexibility. Vanillin can be extracted or synthesized from natural herbs (Zhang et al., 2015). And is a type of aldehyde with a benzene ring that can be used as a renewable alternative to synthetic bio-based materials (Bassett et al., 2020; Geng et al., 2018). In previous work, a vanillo diol (VAN-OH) containing dynamic imine bonds was prepared using vanillin (Sun et al., 2021). The molecule contains benzene ring conjugated structure and double Schiff base structure, which can improve the rigidity of the material (Xu et al., 2019). The dynamic imine bond provides a foundation for the subsequent design of dynamic polyurethane. Moreover, due to the effects of thermal and pH stimuli on imine bonds, polyurethane can be endowed with more functions such as self-healing, reprocessing, antibacterial, and controllable degradation (Xu et al., 2019; Taynton et al., 2016; Luo et al., 2018; Memon et al., 2020; Taynton et al., 2014). In recent years, there have been many research reports on self-healing polyurethane, but there are not many reports on bio-based self-healing polyurethane, and there is little research on the chain structure and properties of bio-based self-healing polyurethane (Gu and Wu, 2018). Possible reasons include the relatively complex chemical structure of bio based monomers, and the significant differences in synthesized bio based polyurethane, making it difficult to explore the relationship between its molecular structure and self-healing performance. Balancing the repair efficiency and mechanical properties of self-healing materials has always been one of the difficulties in self-healing materials, and adding biomass components poses a greater challenge to bio-based self-healing materials. The hydrogen bonding and microphase separation in polyurethane have a certain impact on the movement of molecular segments and the macroscopic repair of materials (Javni et al., 2015; Hesketh et al., 1980).

In this work, a series of vanillin-based polyurethanes were prepared by changing the ratio of soft and hard segments and the relationship between the structure and properties of polyurethane was studied. A biobased polyurethane material with high tensile strength and rapid body temperature repair has been prepared. A bio-based polyurethane material with high tensile strength and rapid body temperature healing has been obtained.

2 Material and methods

2.1 Materials

Vanillin (VAN, 99%), m-xylylenediamine (MXDA, 99%), Polytetramethylene Ether Glycol (PTMG), 4,4′-Dicyclohexylmethane diisocyanate (HMDI, >90%), 1,4-Butanediol (BDO, 99%), dibutyltin dilaurate (DBTDL, 95%) were all purchased from Aladdin. PTMG and BDO need to be vacuum dired before using. Others were used without further purification. The molecular weight of Polytetramethylene Ether Glycol is 2000. Dichloromethane and Dimethylformamide (DMF) were purchased from Saen Chemical Technology Co. Ltd. and used directly.

2.2 Preparation of vanillin based temperature self-healing polyurethane

Vanillin diol (VAN-OH) containing dynamic imine bonds was prepared starting from the bio-based material vanillin, which as a bio-based chain extender for drying and backup. The synthesis of VAN-OH was detailed in our previous work (Sun et al., 2021).

Before conducting the synthesis experiment, PTMG was in a sealed round bottom flask and dried under vacuum at 120°C for 2 h before use. The two chain extenders BDO and VAN-OH placed in a vacuum oven at 80°C for 24 h in advance, respectively, and then set aside for later use. According to Table 1, a series of vanillin based polyurethanes named VPU1-3 were prepared by changing the ratio of soft and hard segments. The synthesis process of vanillin based polyurethane was divided into two steps. The synthesis process of VPU1 was as an example, the first step is the pre polymerization process: first, HMDI (2.62 g, 10 mmol) and DBTDL (0.3%) were dissolved in 10 mL anhydrous DMF. The mixed solution was placed in a reaction flask protected by argon gas. PTMG (10 g, 5 mmol) was dissolved in 20 mL anhydrous DMF and slowly added to the reaction flask at a constant speed. The isocyanate terminated prepolymer was obtained at 60°C for 1 h.

TABLE 1 Chemical composition, hard segment content, molecular weight and molecular weight distribution, as well as bio-based content of VPUs samples.

Sample	Molar ratio			HSC (%)	M_n (g/mol)	M_w (g/mol)	PDI	Bio-based content (%)
	PTMG	HMDI	VAN-OH					
VPU1	1	2	1	32.3	2.88×10^4	5.18×10^4	1.80	13.7
VPU2	1	3	2	44.6	2.23×10^4	3.77×10^4	1.69	22.3
VPU3	1	4	3	53.3	1.81×10^4	3.13×10^4	1.74	28.3

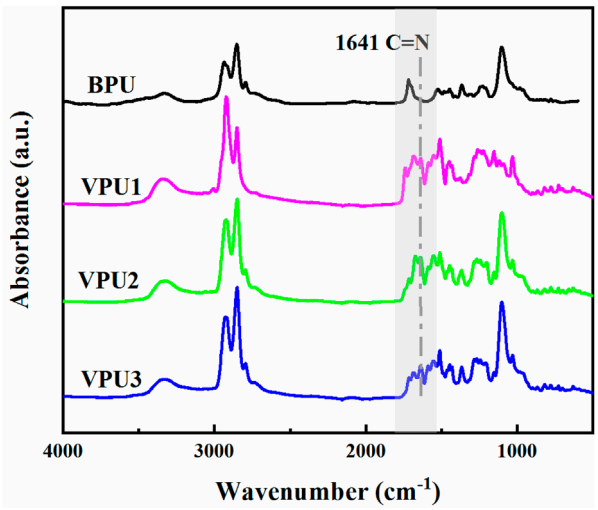

FIGURE 1
FTIR spectra curves of BPU and VPUs.

The second step is the chain extension process: The dried VAN-OH was completely dissolved in 10 mL anhydrous DMF and added into the reaction flask for 30 min under argon atmosphere to obtain a light yellow transparent viscous liquid, vacuum degas for 5 min, and then transfer the reactants to a square PTFE mold. After placing it in a vacuum oven at 60°C and standing for 48 h to completely evaporate the solvent, A transparent film with a thickness of 0.5 mm was obtained (Figure 1). Polyurethane without VAN-OH was prepared using BDO as a chain extender which named BPU as the reference group.

2.3 Characterization methods

2.3.1 Fourier transform infrared spectroscopy (FTIR) testing

The FTIR instrument is the Vertex 70 model from Bruker, Germany. The infrared testing of liquid raw materials adopts the transmission mode, while the infrared testing of VAN-OH and polyurethane films adopts the total reflection mode. The wavenumber range for testing is 4,000~500 cm^{-1}, with a resolution of 2 cm^{-1} and a scanning frequency of 32 times. Diamond is used as a reflective crystal. Using peak fitting software (PeakFit v4.12, peak type: Gaussian Lorenz curve), the infrared peak of C=O in vanillin based polyurethane was divided and calculated to study the degree of hydrogen bonding in the sample.

2.3.2 Gel permeation chromatography (GPC)

GPC, The volume exclusion method is used to test the molecular weight and molecular weight distribution of polyurethane. The GPC instrument is the British PL-GPC 120 model. The number average molecular weight (M_n), weight average molecular weight (M_w), and molecular weight distribution coefficient (PDI) of polyurethane samples were obtained through GPC testing. First, calibrate the molecular weight using standard polystyrene. The concentration of the test sample is 3 mg/mL, the test solvent is DMF, the test temperature is 80°C, and the test flow rate is 1 mL/min.

2.3.3 Thermogravimetric analysis (TGA)

Choose the Toled O-type TGA instrument from Mettler, Switzerland. All samples were tested under N_2 atmosphere, with a sample weight of 3 mg, a heating rate of 10°C min^{-1}, and a testing temperature range of 30~800°C.

2.3.4 Dynamic thermodynamic analysis (DMA)

By using the temperature rise mode of DMA to determine the polymer segment mobility of the sample, important polymer information such as Tg, storage modulus (E′), loss modulus (E″), and loss factor (Tanδ) can be obtained. DMA instrument selected is the Q800 model from TA Corporation in the United States. The testing mode is small strain tensile mode, and the sample is a rectangular spline of 20 mm × 3 mm × 0.5 mm. The testing temperature range of the sample is −80~120°C, and the heating rate is 3°C min^{-1}. During the testing process, the tensile strain of the sample is controlled in the linear strain zone, with amplitude and frequency of 5 μm and 1 Hz, respectively.

2.3.5 Stress relaxation test

The stress relaxation of the sample was performed using the DHR3 rheometer from TA Corporation in the United States. Using the, ETC., mode of the rheometer, parallel throwable aluminum plates were used with a sample diameter of 8 mm and a thickness of approximately 0.5 mm. The strain rate tested in the stress relaxation experiment is 5%, and the stress relaxation time varies linearly with an observation time of 1,500 s. Preheat and hold

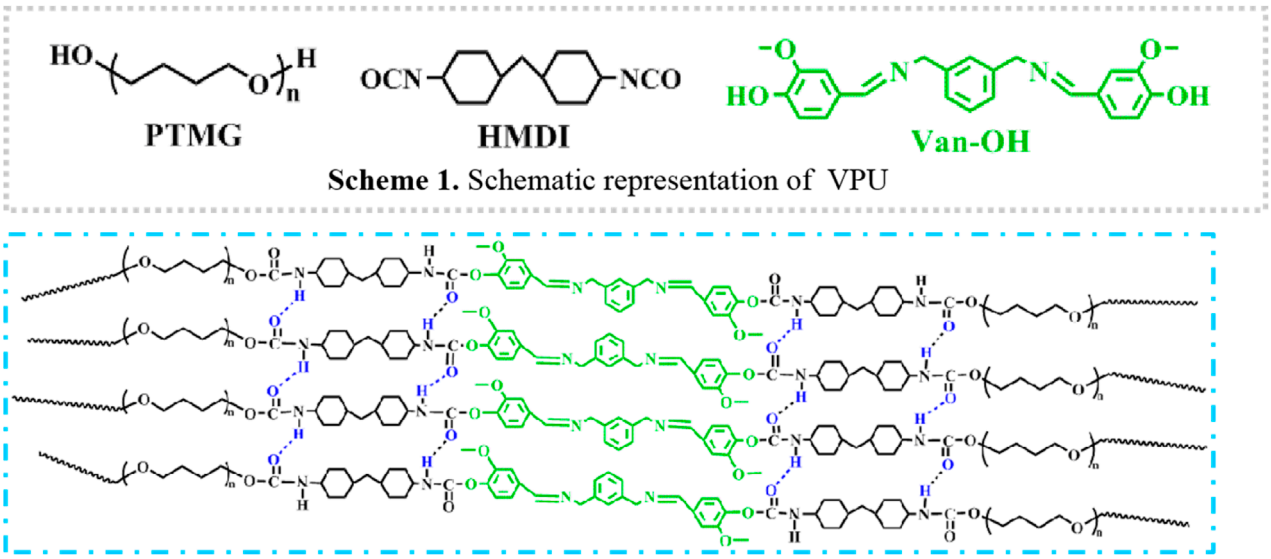

Scheme 1. Schematic representation of VPU

FIGURE 2
Composition and molecular schematic of VPUs.

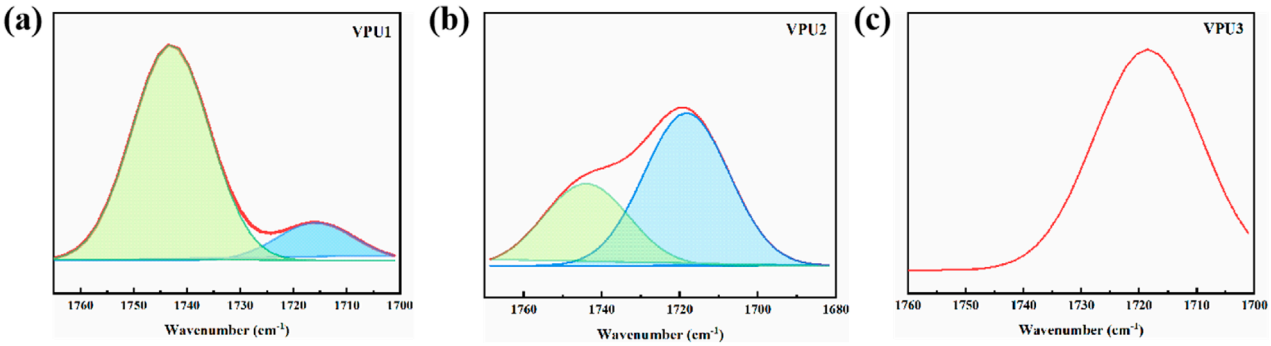

FIGURE 3
The attribution of infrared spectra band for stretching vibration of C=O in CVIPUs by peak separation method. **(A)** VPU1; **(B)** VPU2; **(C)** VPU3.

at each temperature for 3 min before testing. Arrhenius equation: $\ln \tau^* = \ln \tau_0 + E_a/RT$; In the formula, Ea is the relaxation activation energy of the polymer, R is the universal gas constant, τ^* is the characteristic relaxation time, and the time for stress relaxation to 1/e of the initial stress. Based on the relaxation time and temperature in the stress relaxation curve of the material, the Arrhenius equation can be used to fit and calculate the relaxation activation energy of the polymer (Van Zee and Nicolaÿ, 2020; Chen et al., 2018).

2.3.6 Frequency scanning test

The variable temperature frequency scanning test of samples was conducted using the DHR3 rheometer from TA Corporation in the United States. The strain was set in the linear deformation zone of the sample at 5%, and the sample was subjected to frequency scanning at 30°C, 40°C, 50°C, 60°C, and 70°C using a stepwise heating method. The frequency scanning range was 100~0.01 rad s^{-1}. Mechanical performance testing The stress-strain test of the sample at room temperature was conducted using the Instron 1,121 universal testing machine from the United States. Cut the sample into dumbbell shaped strips of 35 mm × 2 mm × 0.5 mm using a standard cutter, with a tensile rate of 50 mm min^{-1}, and conduct 5 tensile tests on each sample.

2.3.7 Water contact angle experiment

Test the hydrophilicity and hydrophobicity of the sample surface through water contact angle experiments at room temperature. The instrument is the Drop Shape Analyzer DSA100 model from Kruss, Germany. The sample size is 10 mm × 10 mm × 0.5 mm. The sample is horizontally fixed on the platform, and a drop of deionized water is dropped vertically. After 1 min, the state of the water droplet on the surface of the sample is recorded by taking a photo with a digital camera, and the instrument automatically calculates the value of the water contact angle. The water contact angle of each sample shall be tested at least 3 times, and the average value shall be taken as the final water contact angle of the sample surface.

TABLE 2 Curve fitting results for infrared spectra analysis of C=O hydrogen bonds degree of VPUs.

Sample	H-bond of carbamate		Free of carbamate		Degree of H-bond (%)
	Wavenumber (cm^{-1})	Integral area	Wavenumber (cm^{-1})	Integral area	
VPU1	1716	0.413	1744	2.399	14.7
VPU2	1718	1.321	1743	0.702	65.3
VPU3	1720	1.337	---	---	100

2.3.8 Small angle X-ray scattering (SAXS)

Small angle X-ray scattering (SAXS) was used to test the degree of microphase separation of polyurethane, and the SAXS instrument was the Nanostar-J model from Bruker, Germany. The resolution of the detector is 105 μm × 105 μm. The scattering angle is 0.1°~0.5°. Bragg formula: 2 days sin θ = nλ; In the formula, d is the interplanar spacing, θ is the θ angle corresponding to the diffraction peak, n is the diffraction order, and λ is the wavelength.

2.3.9 Mechanical performance testing

The stress-strain test of the sample at room temperature was conducted using the Instron 1,121 universal testing machine from the United States. Cut the sample into dumbbell shaped strips of 35 mm × 2 mm × 0.5 mm using a standard cutter, with a tensile rate of 50 mm min^{-1}, and conduct 5 tensile tests on each sample.

2.3.10 Scratch repair experiment

Polarized microscope (POM) was used to observe the scratch repair on the surface of the sample, and the POM instrument was the DM2500P model from Leica, Germany. Select the transmission mode for the light source direction, use a clean double-sided blade to create 5 μm × 15 μm scratches on the surface of the film material, and then place the sample on the Linkam hot stage matched with the microscope. Set the hot stage temperature to the corresponding testing temperature, record the time, observe the scratch repair process with the microscope, and take photos for recording.

2.3.11 Stretch healing experiment

The sample was cut form middle and spliced together. Next the spliced sample was placed in a 36°C oven for healing. Healing efficiency:

$$\text{Healing Efficiency } (\%) = \frac{\sigma \text{ of healing sample}}{\sigma \text{ of original sample}} \times 100\%$$

3 Results and discussion

Vanillin and meta phenylenediamine can be converted into Vanillin Glycol Monomer (VAN-OH) through a simple amine aldehyde condensation reaction. VAN-OH contains dihydroxy groups and is a small molecule diol with vanillin groups, which can be used as a chain extender for polyurethane. The molecule contains benzene ring conjugated structure and double Schiff base structure, which can improve the rigidity of the material. The dynamic imine bond provides a foundation for the subsequent design of self-healing polyurethanes. Figure 2 shows the infrared spectrum of polyurethane. Compared with BPU, VPUs exhibit a C=N stretching vibration peak at 1,641 cm^{-1} in the infrared, indicating the presence of a large number of imine bonds in VPUs (Sun et al., 2022; Zheng et al., 2018). There are no characteristic peaks of NCO groups at 2270 cm^{-1}, indicating that the NCO groups have fully reacted (Yan et al., 2017). A significant change was also observed in the carbonyl peak position at 1700 cm^{-1}, and a shoulder peak appeared in the C=O peak of VPUs, indicating that the use of benzene ring conjugated chain

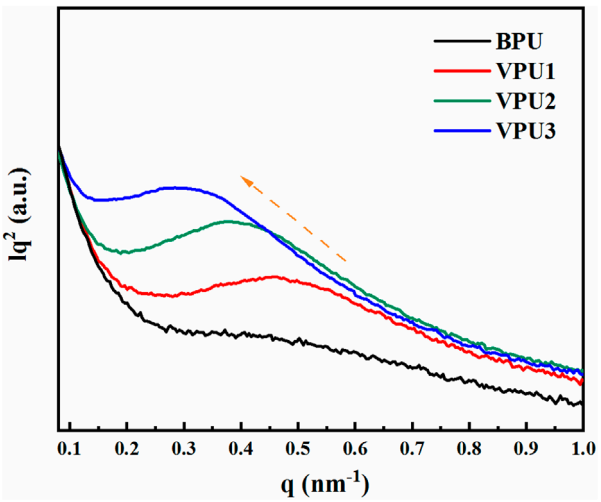

FIGURE 4
SAXS results of BPU and VPUs.

TABLE 3 SAXS results of BPU and VPUs.

Sample	q (nm^{-1})	d (nm)
VPU1	0.46	14
VPU2	0.38	17
VPU3	0.29	22

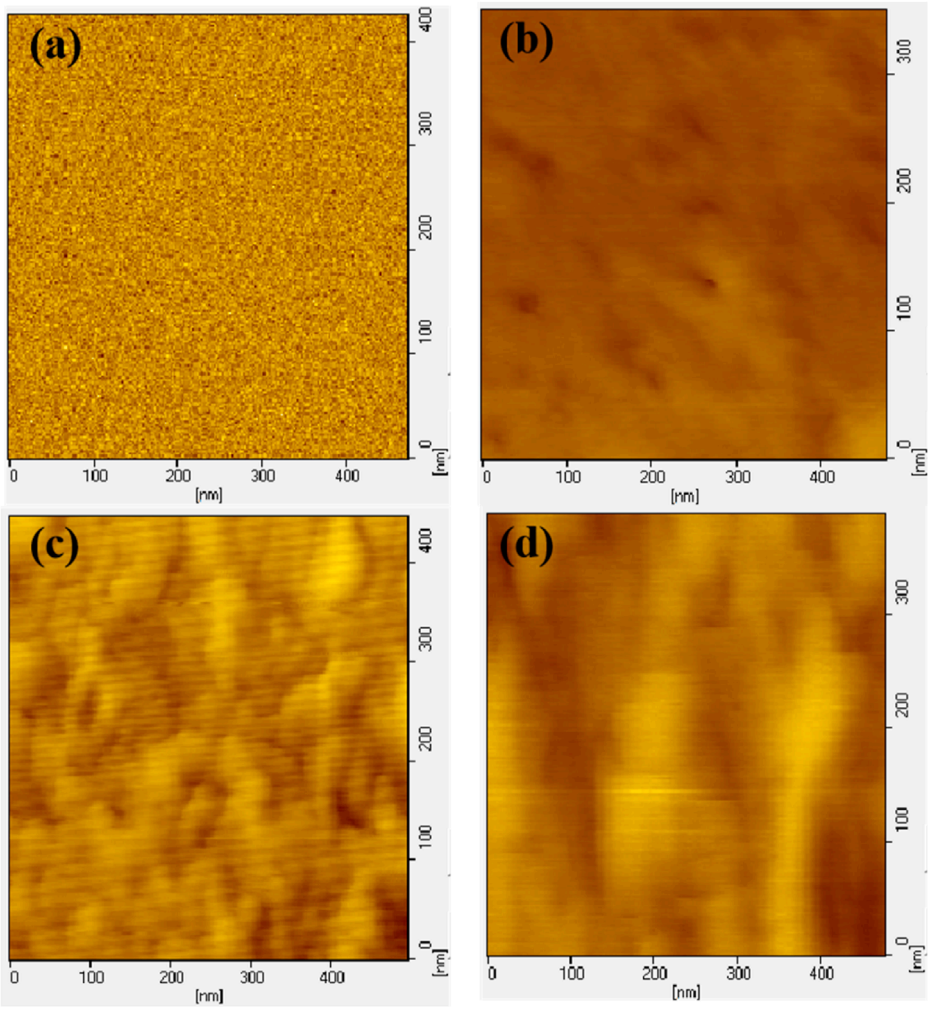

FIGURE 5
AFM phase diagram: **(A)** BPU; **(B)** VPU1; **(C)** VPU2; **(D)** VPU3.

extenders can affect the hydrogen bond changes in polyurethane, and increasing the hard segment content can also affect the hydrogen bond types in the system. C=O in amino esters can form hydrogen bonds, which can cause a shift in the infrared peak position of C=O.

Subsequently, we classified the carbonyl peaks of the amino esters between 1700–1760 cm^{-1}, as shown in Figure 3 and Table 2. We found that with the increase of hard segment content, the content of free hydrogen bonds decreased, the proportion of bound hydrogen bonds increased, and the degree of hydrogen bonding in polyurethane increased. The reason is that the content of VAN-OH in the hard segment will also increase, and the conjugated structure of the benzene ring in vanilla diol will form a more regular stack. The aggregation ability between hard segments shortens the distance between them, making it easier to form hydrogen bonds in the hard segment region.

The rigid segments formed by HMDI and diol chain extension are difficult to undergo microphase separation in the aggregated state of polyurethane. However, due to the increase in the number of benzene rings and the lengthening of the rigid segments, microphase separation may occur in polyurethane elastomers. The small angle scatter plot also indicates that with the increase of hard segment content, the degree of microphase separation of polyurethane is significant. As shown in Figure 4, the scattering peak of BPU between 0.1–1.0 nm^{-1} is not obvious, while the scattering peak of VPUs appears. The scattering vector (q) of VPU1 is 0.46 nm^{-1}. As the hard segment content increases, the scattering vector decreases. The phase spacing (d) can be calculated using the Bragg formula, as shown in Table 3. With the increase of hard segment content, the phase spacing within VPUs increases from 14 nm to 22 nm. This indicates that the degree of phase separation in bio-based polyurethane has increased, and we subsequently verified this by observing the microstructure of polyurethane using atomic force microscopy (AFM) (Scott M. and Sauer, 1997). The phase diagram of polyurethane is shown in Figure 5. We scanned the sample in the range of 500 nm, and the hard segment formed a surface protrusion due to its high cohesive energy. And the corresponding soft segment is the concave part on the surface. When the content of hard segments is small, the soft segments act as continuous phases, while the hard segments act

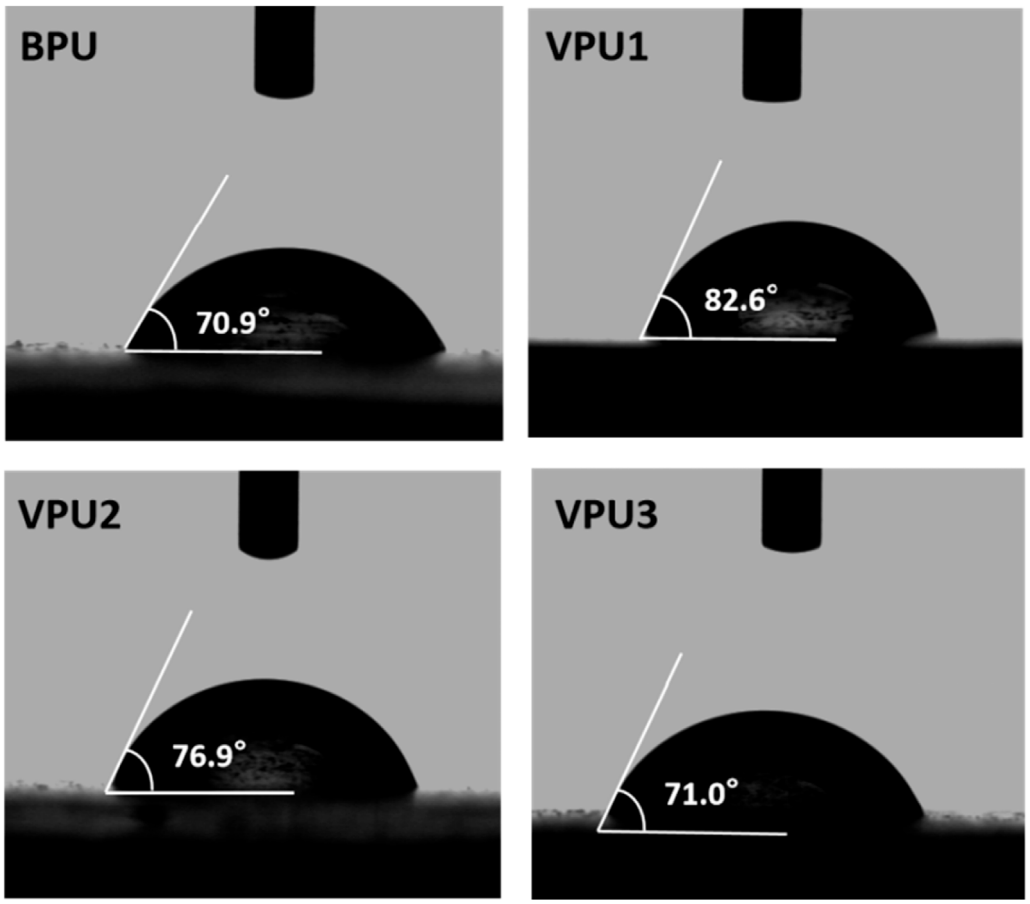

FIGURE 6
Images of water contact angle on surface of different samples.

as dispersed phases. The phase separation in the material is not obvious. The hard segment content in VPU3 is as high as 55.34%. The π - π conjugated structure of VAN-OH and the increased degree of hydrogen bonding promote the aggregation of hard segments, resulting in the maximization of microphase separation in VPU3.

Water contact angle experiments were conducted on the materials, as shown in Figure 6. The water contact angles on all sample surfaces exceeded 70°, but were all less than 90°, indicating a certain degree of hydrophilicity. This is due to the presence of a large number of polar amino ester groups in polyurethane, which increases the surface tension of the material and reduces the contact angle of water on its surface. The water contact angle of VPU1 is the highest, at 82.6°. As the content of hard segments increases, the surface water contact angle of the sample gradually decreases. This is due to the increase in polar groups in the material, which leads to an increase in its hydrophilicity. Due to the conjugated structure of the benzene ring in VAN-OH, its hydrophobicity in VPU is superior to that of aliphatic chain extenders, resulting in a larger surface contact angle of VPU compared to BPU.

The mechanical properties of the sample were characterized (Figure 7; Table 4). The tensile strength of BPU is 14.6 MPa, and the elongation at break is 1,110.4%. The mechanical properties of vanillin based polyurethane vary greatly. As the content of VAN-OH increases, the proportion of hard segments increases, the tensile strength of the material increases, and the elongation at break decreases. VPU3 has a high yield stress, a tensile strength of 29.1 MPa, and a fracture elongation of 229.4%. The increase in the content of rigid functional groups in materials and the degree of microphase separation in polyurethane are closely related to the improvement of their mechanical properties.

As shown in Figures 8A, B represent the thermogravimetric curves and differential thermogravimetric curves of the sample. With the increase of hard segment content, the heat resistance of the sample is improved. The material underwent minor degradation near 200°C, possibly due to residual small molecule vanillodiol in the sample. The thermal weight loss at 340°C can be attributed to the thermal decomposition of amino esters in polyurethane, while the thermal weight loss near 414°C is the degradation of soft segment polyether in polyurethane (Simon et al., 1988). To investigate the segmental motion of polymers, we conducted DMA analysis on the samples. The curves of storage modulus (E′) and loss factor (Tan δ) with temperature are shown in Figures 8C, D. As the content of VAN-OH increases, the proportion of rigid

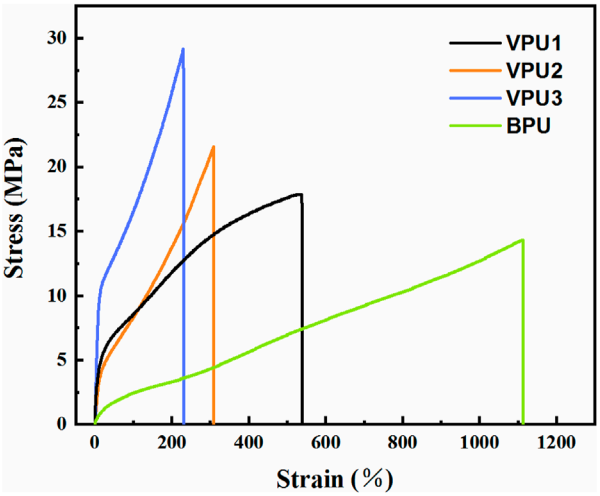

FIGURE 7
Strain-stress curves of VPUs and BPU.

TABLE 4 Mechanical properties of BPU and VPUs.

Sample	Strength (MPa)	Elongation at break (%)
BPU	14.3 ± 0.7	1,111.3 ± 13
VPU1	17.9 ± 0.9	536.6 ± 9
VPU2	21.4 ± 1.4	308.1 ± 5
VPU3	29.1 ± 2.4	229.4 ± 3

segments with benzene rings in polyurethane increases, and the storage modulus of the material gradually increases (Mankar et al., 2019). The temperature corresponding to the peak of the loss factor represents the glass transition temperature of the sample, as shown in Figure 6D. The T_g of all four polyurethanes is below −50°C. It has been proven that PTMG type polyurethane has good flexibility at low temperatures. As the content of hard segments increases, the T_g of polyurethane increases from −60°C to −52°C. At lower temperatures, the chain segments in the soft segment region are more likely to thaw and move from a frozen state, and a large number of hard segments will limit the movement of the soft segments. So the T_g of VPU3 is smaller than that of VPU1. On the side, it reflects that the intermolecular interactions within VPU are stronger, and the content of hard segments increases, acting as physical cross-linking points within polyurethane, resulting in a higher T_g of the material.

Stress relaxation experiments were conducted on 4 types of polyurethanes at different temperatures to analyze the mobility of polymer molecular chains. As shown in Figure 9, as the temperature increases, the movement speed of all polymer segments accelerates and the relaxation time becomes shorter. When the temperature of BPU is below 60°C, it is difficult for the chain segment to relax to 1/e. And polyurethane with added vanillin diol has a stronger temperature dependence on its stress relaxation ability. The higher the content of VAN-OH, the shorter the stress relaxation time of the polymer, which is due to the dynamic imine bond exchange triggered by the increase in temperature (Xu et al., 2020). The relaxation time and temperature of VPU1, VPU2, and VPU3 satisfy the Arrhenius formula, and their relaxation activation energies (Ea) are calculated to be 55.87, 55.45, and 50.96 kJ mol^{-1}, respectively, through formula fitting. We found that as the content of hard segments in VPU increases, the degree of phase separation also increases. However, this phenomenon does not hinder the overall movement of the chain segments. With the increase of hard segment content, the degree of hydrogen bonding increases, similar to a phase locking mechanism, which brings the hard segment regions closer together, making it easier for the imine bonds in vanillin to undergo dynamic exchange and promoting the overall relaxation movement of the polymer (Fan et al., 2020). So the relaxation activation energy of the material has decreased, indicating that the addition of VAN-OH improves the overall connectivity of the polymer.

Figure 10 shows the variation of storage modulus and loss modulus of four types of polyurethane with frequency at different temperatures. BPU exhibits solid behavior within the temperature range of 30~80°C, where G ′remains above G″ throughout the entire frequency range. As the temperature increases, transition crossing points (G′ = G″) from solid behavior to liquid behavior appear in the sweep frequency curves of VPUs, and as the temperature increases, the crossing points move to higher frequencies. This is because chains have greater fluidity at higher temperatures, and in addition, polymers are more prone to motion and relaxation of molecular chains at lower shear frequencies, corresponding to larger time scales (Zhou et al., 2017). Therefore, materials exhibit liquid like behavior at low frequencies, and even at lower temperatures, solid-liquid intersections are more likely to occur at low frequencies (Nevejans et al., 2019). VPU1 showed a gel sol transition at the low frequency of 60°C, VPU2 shows a transition point at 50°C, and VPU3 shows a solid-liquid transition point at a lower temperature (40°C), indicating that the chain segment mobility of the polymer from high to low is VPU3>VPU2>VPU1>BPU, which is also consistent with the stress relaxation experiment results of the material.

Due to the solid-liquid transition point observed in the low-frequency region of VPU3 at 40°C, we attempted to test the scratch repair ability of the sample at 36°C (human body temperature). Observation using a polarizing microscope (POM) can visually demonstrate the scratch self-healing properties of the material. Place the damaged sample on a heating table at 36°C to observe the self-healing behavior of the material. As shown as Figure 11, It can be seen that the scratch width of VPU1 narrows after 10 min, and the scratch of VPU3 has almost disappeared. After 20 min, the scratch width on the surface of VPU1 gradually decreases; The surface scratches of VPU3 have completely healed. As for the reference group sample BPU, due to the absence of dynamic keys, its surface scratches did not undergo any changes, indicating that BPU does not have self-healing ability. The above phenomenon indicates that VPU3 has the best segment movement ability, which enables it to achieve scratch self repair at lower temperatures.

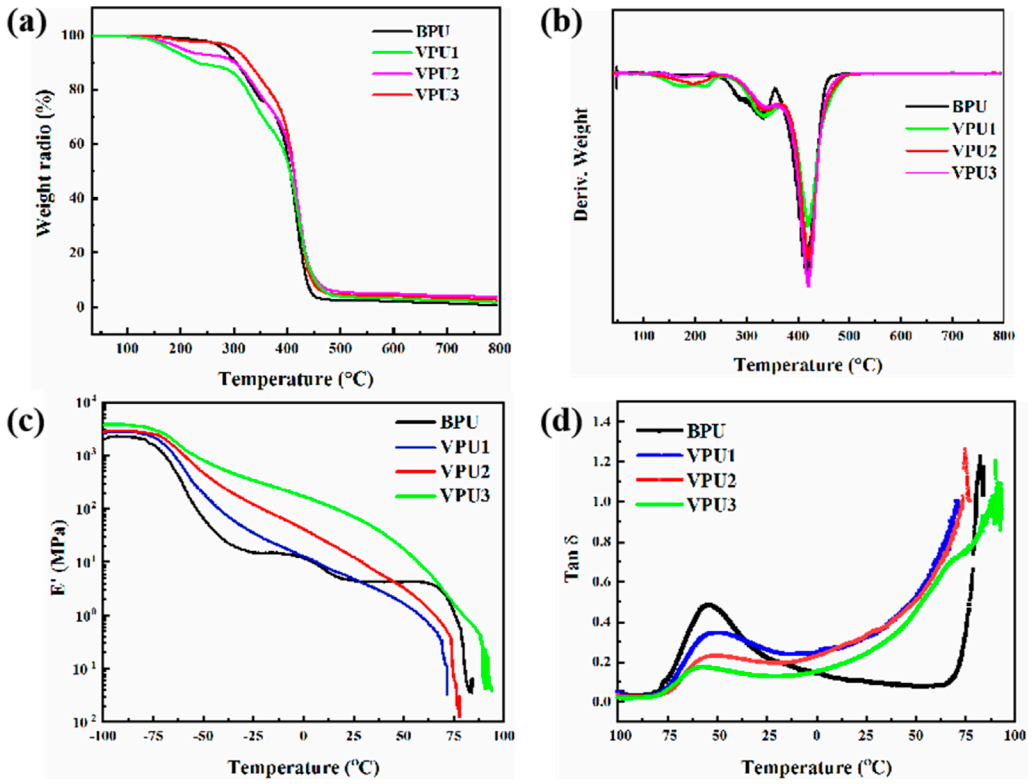

FIGURE 8
(A) TGA curves of BPU and VPUs **(B)** DTG curves of BPU and VPUs **(C)** Variation curves of storage modulus with temperature **(D)** Variation curves of Tanδ with temperature.

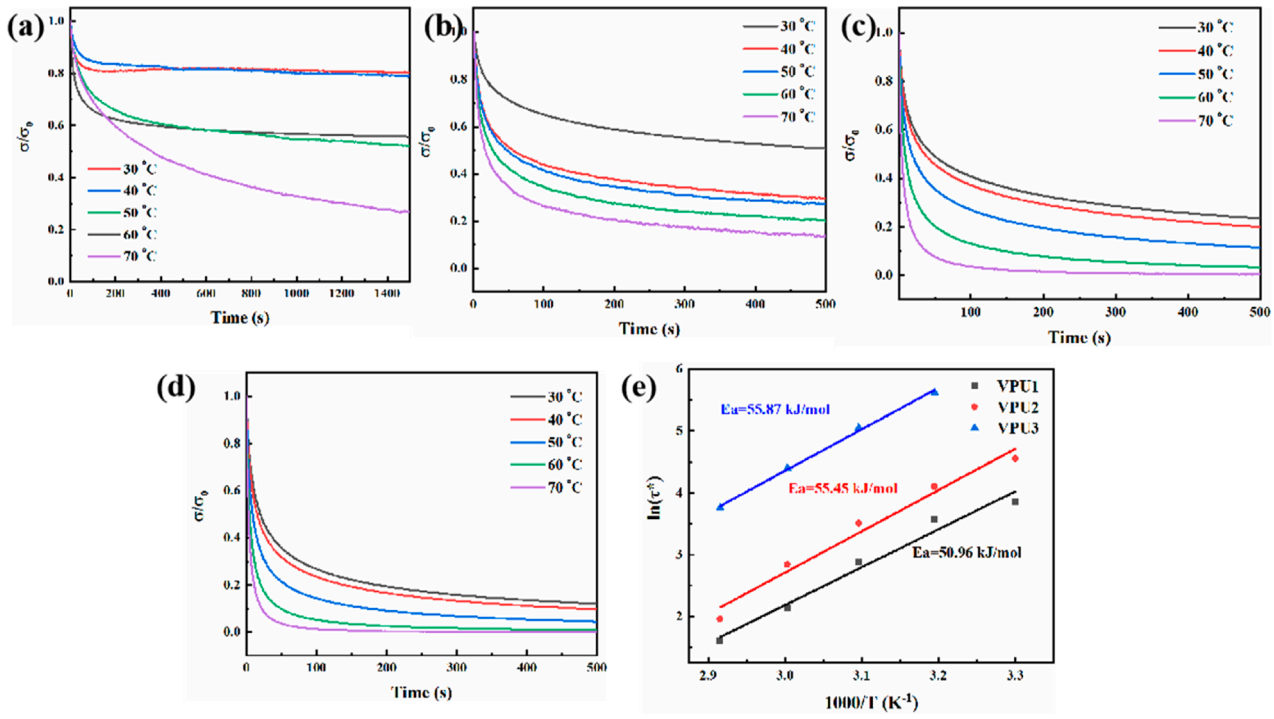

FIGURE 9
Stress relaxation curves of sample at different temperatures **(A)** BPU; **(B)** VPU1; **(C)** VPU2; **(D)** VPU3. **(E)** Fitted Arrhenius equation of VPUs according to the experimental data.

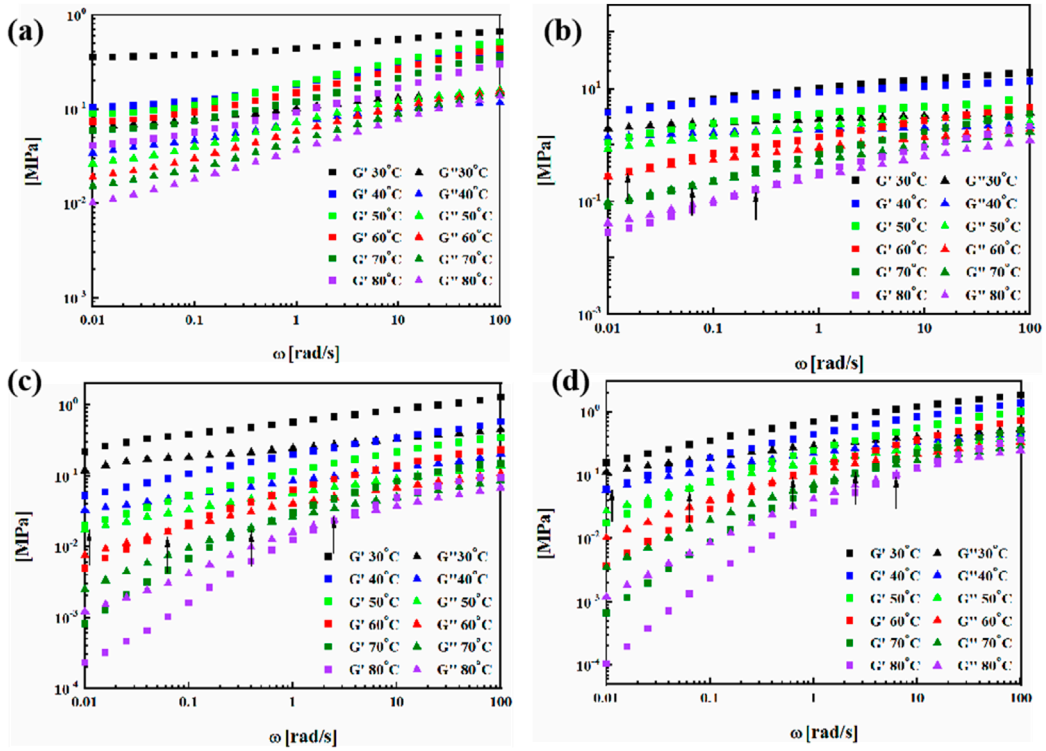

FIGURE 10
G′ and G″ values between 0.01 and 100 Hz at diffffferent temperatures of **(A)** BPU; **(B)** VPU1; **(C)** VPU2; **(D)** VPU3.

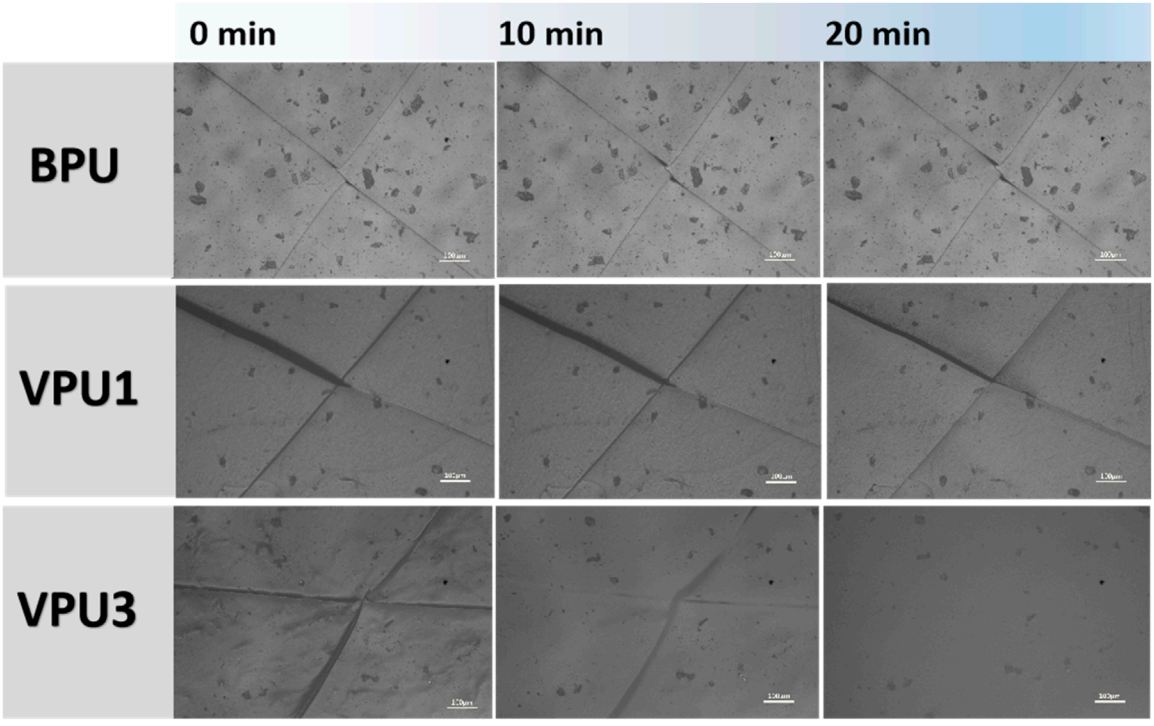

FIGURE 11
Optical microscopy images of scratch healing test results over time at 36°C.

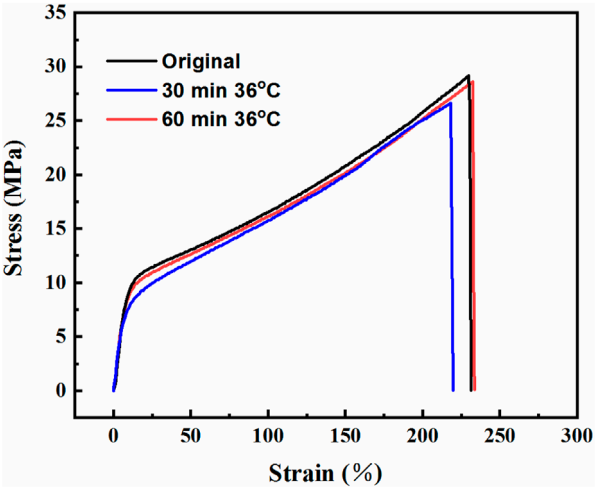

FIGURE 12
Strain-stress curves at different healing times and conditions obtained for VPU3.

Then, tensile tests were performed on the VPU3 sample after cutting and healing (heal at 36°C) to quantitatively evaluate the healing properties of VPU3 (Figure 12). VPU3 has excellent healing properties, and it can recover to 98% of its original stress in 20 min at 36°C. The hydrogen bond formed between the carbamate groups generated by the reaction provides a fraction of self-healing efficiency. The hydrogen bond makes the cut surface bite tight so that the dynamic exchange reaction of Imine bond can proceed more fully at the cut surface.

Then, tensile tests were performed on the VPU3 sample after cutting and healing (heal at 36°C) to quantitatively evaluate the healing properties of VPU3. As the healing time prolongs, the healing efficiency improves. The samples has excellent healing properties, and it can recover to 97% of its original stress in 60 min at 36°C and recover to nearly 100% of its original strain. The high mobility of soft segments at lower temperatures and the promotion of dynamic exchange of imine bonds through regular hydrogen bond arrangement synergistically contribute to the self-healing of VPU3 samples at body temperature.

4 Conclusion

In this work, a series of vanillin based polyurethanes (VPUs) composed of HMDI, PTMG and vanillin based chain extenders containing imine bonds were synthesized. By changing the ratio of soft and hard segments, the degree of micro phase separation and hydrogen bonding of the material can be regulated, indirectly affecting the thermal, mechanical, and hydrophilic properties of the material. Rheological experiments showed that VPUs with VAN-OH has faster chain segment relaxation ability and dynamic imine bonds can undergo rapid exchange at higher temperatures, making the material more prone to solid-liquid transition. With the increase of hard segment content, the chain segment relaxation ability can be enhanced, VPU3 not only has excellent mechanical properties (fracture strength 29.1 MPa, fracture elongation 229.4%), but also has strong self-healing ability. It can quickly recover to 97% of its original strength in 1 h at body temperature.

Data availability statement

The original contributions presented in the study are included in the article, further inquiries can be directed to the corresponding authors.

Author contributions

MF: Resources, Writing–original draft. JH: Data curation, Writing–original draft. XZ: Writing–original draft, Formal Analysis. CW: Writing–original draft, Methodology. YL: Writing–original draft, Software, Supervision, Validation, Writing–review and editing. JN: Writing–review and editing, Formal Analysis, Resources, Supervision. YS: Writing–review and editing, Conceptualization, Writing–original draft. DY: Supervision, Validation, Writing–review and editing. XJ: Formal Analysis, Supervision, Validation, Writing–original draft, Writing–review and editing.

Funding

The author(s) declare that no financial support was received for the research, authorship, and/or publication of this article.

Conflict of interest

Authors MF, JH, YL, and JN were employed by Pipe China West Pipeline Company. Author CW was employed by Pipe China Gansu Pipeline Company. Author XJ was employed by Lianyungang Jingwei Composite New Materials Co., Ltd.

The remaining authors declare that the research was conducted in the absence of any commercial or financial relationships that could be construed as a potential conflict of interest.

Generative AI statement

The author(s) declare that no Generative AI was used in the creation of this manuscript.

Publisher's note

References

Akindoyo, J. O., Beg, M. D. H., Ghazali, S., Islam, M. R., Jeyaratnam, N., and Yuvaraj, A. R. (2016). Polyurethane types, synthesis and applications-a review. *RSC Adv.* 6 (115), 114453–114482. doi:10.1039/c6ra14525f

Alabiso, W., and Schlogl, S. (2020). The impact of vitrimers on the industry of the future: chemistry, properties and sustainable forward-looking applications. *Polymers* 12 (8), 1660. doi:10.3390/polym12081660

Bassett, A. W., Honnig Amy, E., Breyta, C. M., Dunn, I. C., La Scala, J. J., and Stanzione, J. F., III (2020). Vanillin-based resin for additive manufacturing. *ACS Sustain. Chem. and Eng.* 8 (14), 5626–5635. doi:10.1021/acssuschemeng.0c00159

Chen, J., Hu, D., Li, Y., Zhu, J., Du, A. K., and Zeng, J. B. (2018). Castor oil-based high performance and reprocessable poly(urethane urea) network. *Polym. Test.* 70, 174–179. doi:10.1016/j.polymertesting.2018.07.004

Chen, T., Wu, H., Zhang, W., Li, J., and Liu, F. (2023). A sustainable body-temperature self-healing polyurethane nanocomposite coating with excellent strength and toughness through optimal hydrogen-bonding interactions. *Prog. Org. Coatings* 185, 107876. doi:10.1016/j.porgcoat.2023.107876

Diesendruck, C. E., Sottos, N. R., Moore, J. S., and White, S. R. (2015). Biomimetic self-healing. *Angewandte Chemie Int. Edtion Engl.* 54 (36), 10428–10447. doi:10.1002/anie.201500484

Dong, X., Ren, J., Duan, Y., Wu, D., Lin, L., Shi, J., et al. (2021). Preparation and properties of green UV-curable itaconic acid cross-linked modified waterborne polyurethane coating. *J. Appl. Polym. Sci.* 139, e52042. doi:10.1002/app.52042

Fan, W., Jin, Y., Shi, L., Zhou, R., and Du, W. (2020). Developing visible-light-induced dynamic aromatic Schiff base bonds for room-temperature self-healable and reprocessable waterborne polyurethanes with high mechanical properties. *J. Mater. Chem. A* 8 (14), 6757–6767. doi:10.1039/c9ta13928a

Geng, H., Wang, Y., Yu, Q., Gu, S., Zhou, Y., Xu, W., et al. (2018). Vanillin-based polyschiff vitrimers: reprocessability and chemical recyclability. *ACS Sustain. Chem. and Eng.* 6 (11), 15463–15470. doi:10.1021/acssuschemeng.8b03925

Gu, L., and Wu, Q. (2018). Recyclable bio-based crosslinked polyurethanes with self-healing ability. *J. Appl. Polym. Sci.* 135 (21), 46272. doi:10.1002/app.46272

Hesketh, T. R., Van Bogart, J. W. C., and Cooper, S. L. (1980). Differential scanning calorimetry analysis of morphological changes in segmented elastomers. *Polym. Eng. Sci.* 20, 190–197. doi:10.1002/pen.760200304

Javni, I., Bilić, O., Bilić, N., Petrović, Z. S., Eastwood, E. A., Zhang, F., et al. (2015). Thermoplastic polyurethanes with controlled morphology based on methylenediphenyldiisocyanate/isosorbide/butanediol hard segments. *Polym. Int.* 64 (11), 1607–1616. doi:10.1002/pi.4960

Jiang, C., Zhang, L., Yang, Q., Huang, S., Shi, H., Long, Q., et al. (2021). Self-healing polyurethane-elastomer with mechanical tunability for multiple biomedical applications *in vivo*. *Nat. Commun.* 12 (1), 4395. doi:10.1038/s41467-021-24680-x

Li, W., Dong, B., Yang, Z., Xu, J., Chen, Q., Li, H., et al. (2018). Recent advances in intrinsic self-healing cementitious materials. *Adv. Mater.* 30 (17), e1705679. doi:10.1002/adma.201705679

Luo, C., Lei, Z., Mao, Y., Shi, X., Zhang, W., and Yu, K. (2018). Chemomechanics in the moisture-induced malleability of polyimine-based covalent adaptable networks. *Macromolecules* 51 (23), 9825–9838. doi:10.1021/acs.macromol.8b02046

Maeda, T., Otsuka, H., and Takahara, A. (2009). Dynamic covalent polymers: reorganizable polymers with dynamic covalent bonds. *Prog. Polym. Sci.* 34 (7), 581–604. doi:10.1016/j.progpolymsci.2009.03.001

Mankar, S. V., Garcia Gonzalez, M. N., Warlin, N., Valsange, N. G., Rehnberg, N., Lundmark, S., et al. (2019). Synthesis, Life cycle assessment and polymerization of a vanillin-based spirocyclic diol toward polyesters with increased glass-transition temperature. *ACS Sustain. Chem. and Eng.* 7 (23), 19090–19103. doi:10.1021/acssuschemeng.9b04930

Memon, H., Liu, H., Rashid, M. A., Chen, L., Jiang, Q., Zhang, L., et al. (2020). Vanillin-based epoxy vitrimer with high performance and closed-Loop recyclability. *Macromolecules* 53 (2), 621–630. doi:10.1021/acs.macromol.9b02006

Nevejans, S., Ballard, N., Fernández, M., Reck, B., and Asua, J. M. (2019). Flexible aromatic disulfide monomers for high-performance self-healable linear and cross-linked poly(urethane-urea) coatings. *Polymer* 166, 229–238. doi:10.1016/j.polymer.2019.02.001

Nevejans, S., Ballard, N., Miranda, J. I., Reck, B., and Asua, J. M. (2016). The underlying mechanisms for self-healing of poly(disulfide)s. *Phys. Chem. Chem. Phys.* 18 (39), 27577–27583. doi:10.1039/c6cp04028d

Ratwani, C. R., Kamali, A. R., and Abdelkader, A. M. (2023). Self-healing by Diels-Alder cycloaddition in advanced functional polymers: a review. *Prog. Mater. Sci.* 131, 101001. doi:10.1016/j.pmatsci.2022.101001

Scott M., R., and Sauer, B. B. (1997). Tapping-mode AFM studies using phase detection for resolution of nanophases in segmented polyurethanes and other block copolymers. *Macromolecules* 30, 8314–8317. doi:10.1021/ma970350e

Simon, J., Barla, F., Kelemen-Haller, A., Farkas, F., and Kraxne, M. (1988). Thermal stability of polyurethanes. *Chromatographia* 25, 99–106. doi:10.1007/bf02259024

Su, Z., Huang, S., Wang, Y., Ling, H., Yang, X., Jin, Y., et al. (2020). Robust, high-barrier, and fully recyclable cellulose-based plastic replacement enabled by a dynamic imine polymer. *J. Mater. Chem. A* 8 (28), 14082–14090. doi:10.1039/d0ta02138e

Sun, Y., Sheng, D., Wu, H., Tian, X., Xie, H., Shi, B., et al. (2021). Bio-based vitrimer-like polyurethane based on dynamic imine bond with high-strength, reprocessability, rapid-degradability and antibacterial ability. *Polymer* 233, 124208. doi:10.1016/j.polymer.2021.124208

Sun, Y., Tian, X., Xie, H., Shi, B., Zhong, J., Liu, X., et al. (2022). Reprocessable and degradable bio-based polyurethane by molecular design engineering with extraordinary mechanical properties for recycling carbon fiber. *Polymer* 258, 125313. doi:10.1016/j.polymer.2022.125313

Taynton, P., Yu, K., Shoemaker, R. K., Jin, Y., Qi, H. J., and Zhang, W. (2014). Heat-or water-driven malleability in a highly recyclable covalent network polymer. *Adv. Mater.* 26 (23), 3938–3942. doi:10.1002/adma.201400317

Taynton, P., Zhu, C., Loob, S., Shoemaker, R., Pritchard, J., Jin, Y., et al. (2016). Re-healable polyimine thermosets: polymer composition and moisture sensitivity. *Polym. Chem.* 7 (46), 7052–7056. doi:10.1039/c6py01395c

Van Zee, N. J., and Nicolaÿ, R. (2020). Vitrimers: permanently crosslinked polymers with dynamic network topology. *Prog. Polym. Sci.* 104, 101233. doi:10.1016/j.progpolymsci.2020.101233

Wu, H., Liu, X., Sheng, D., Zhou, Y., Xu, S., Xie, H., et al. (2021). High performance and near body temperature induced self-healing thermoplastic polyurethane based on dynamic disulfide and hydrogen bonds. *Polymer* 214, 123261. doi:10.1016/j.polymer.2020.123261

Xu, X., Ma, S., Wu, J., Yang, J., Wang, B., Wang, S., et al. (2019). High-performance, command-degradable, antibacterial Schiff base epoxy thermosets: synthesis and properties. *J. Mater. Chem. A* 7 (25), 15420–15431. doi:10.1039/c9ta05293c

Xu, Y., Odelius, K., and Hakkarainen, M. (2020). Photocurable, thermally reprocessable, and chemically recyclable vanillin-based imine thermosets. *ACS Sustain. Chem. and Eng.* 8 (46), 17272–17279. doi:10.1021/acssuschemeng.0c06248

Yan, P., Zhao, W., Fu, X., Liu, Z., Kong, W., Zhou, C., et al. (2017). Multifunctional polyurethane-vitrimers completely based on transcarbamoylation of carbamates: thermally-induced dual-shape memory effect and self-welding. *RSC Adv.* 7 (43), 26858–26866. doi:10.1039/c7ra01711a

Yan, X., Yang, K., Song, B., Li, L., Han, L., and Zhang, R. (2024). Polyurethane with long hard segment for self-healing in blood environment around body temperature. *Chem. Eng. J.* 487, 150509. doi:10.1016/j.cej.2024.150509

Zhang, C., Madbouly, S. A., and Kessler, M. R. (2015). Renewable polymers prepared from vanillin and its derivatives. *Macromol. Chem. Phys.* 216 (17), 1816–1822. doi:10.1002/macp.201500194

Zhang, Y., Yu, Y., Zhao, X., Yang, X., Yu, R., Zhang, Y., et al. (2021). A high strength but fast fracture-self-healing thermoplastic elastomer. *Macromol. Rapid Commun.* 42 (14), e2100135. doi:10.1002/marc.202100135

Zheng, H., Liu, Q., Lei, X., Chen, Y., Zhang, B., and Zhang, Q. (2018). A conjugation polyimine vitrimer: fabrication and performance. *J. Polym. Sci. Part A Polym. Chem.* 56 (22), 2531–2538. doi:10.1002/pola.29232

Zhou, Y., Goossens Johannes, G. P., Sijbesma Rint, P., and Heuts, J. P. A. (2017). Poly(butylene terephthalate)/glycerol-based vitrimers via solid-state polymerization. *Macromolecules* 50 (17), 6742–6751. doi:10.1021/acs.macromol.7b01142